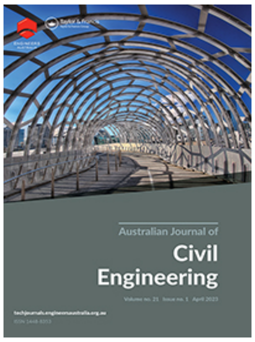


Australian Journal of Civil Engineering

ISSN: (Print) (Online) Journal homepage: https://www.tandfonline.com/loi/tcen20


# Role of Geogrid reinforcement and its diverse applications in the geotechnical engineering and allied fields: a-state-of-the-art review


**Kiran Prakash K, Deendayal Rathod & Kasinathan Muthukkumaran**



**To cite this article:** Kiran Prakash K, Deendayal Rathod & Kasinathan Muthukkumaran (2023): Role of Geogrid reinforcement and its diverse applications in the geotechnical engineering and allied fields: a-state-of-the-art review, Australian Journal of Civil Engineering, DOI: 10.1080/14488353.2023.2205674

**To link to this article:** https://doi.org/10.1080/14488353.2023.2205674

Published online: 09 May 2023.

AUSTRALIAN JOURNAL OF CIVIL ENGINEERING
https://doi.org/10.1080/14488353.2023.2205674



# Role of Geogrid reinforcement and its diverse applications in the geotechnical engineering and allied fields: a-state-of-the-art review

Kiran Prakash K, Deendayal Rathod and Kasinathan Muthukkumaran

Department of Civil Engineering, National Institute of Technology (NIT), Tiruchirappalli, Tamil Nadu, India

**ABSTRACT**

Soils and geosynthetics are terms used interchangeably whenever the physical and mechanical properties of the soil are unlikely to sustain the load coming over it. Several studies have been undertaken to determine the benefits of using geosynthetic products instead of conventional procedures such as stone columns, jet grouting, soil nailing, and so on. As far as geotechnical applications are concerned, geogrid is the most widely utilised polymeric product. This paper provided an overview of geogrid's numerous applications, including pavements, airport runways, railroads, building foundations, MSE walls, bridge embankments, and landfills. Furthermore, this bibliometric analysis has revealed the important laboratory model experiments done on geogrids as well as numerical finite element and finite difference model analysis. An overview of several case studies involving geogrid reinforcement in large projects was also documented; the review also discussed the present trends and opportunities for future development of new geogrid reinforcement technologies within the same section of the literature collection to have better clarity for comparison.

**ARTICLE HISTORY**
Received 29 September 2022
Accepted 18 April 2023

**KEYWORDS**
Review; geogrid reinforcement; pavement applications; footing applications; reinforced soil slopes; reinforced MSE wall; reinforcement mechanism

## 1. Introduction

Engineering soil is weak in tension. After extensive research, we deduced that the incorporation of a tensile material into engineered soil would overcome the weakness of the soil. Geogrid is a tensile material, and owing to its economy, ease of construction, and environmentally friendly nature, they are abundantly used to reinforce poor soil. The performance and load-carrying capacity of the soil-geogrid composite system is enhanced by the interaction between soil and geogrid reinforcement with a high stiffness ratio. The stiffness difference between soil and geogrid has an important effect on shear stress mobilisation along the geogrid, which increases the shear strength of reinforced soil, popularly known as the stiffening effect (Halder and Chakraborty 2019; Tutumluer, Huang, and Bian 2012). The tensile force of the geogrid can be increased even further by using prestressing geogrid concepts (Lackner, Bergado, and Semprich 2013). The aperture size, mechanical properties of the geosynthetic product, and soil used also positively affect increased load-carrying capacity and reduced irrecoverable deformation.

Weak soils with very low shear strengths cover the majority of India's land. As a result, the only method of construction was the time-consuming excavation of weak soil and replacement with improved soil. As an alternative, a 1- to 2-m-thick sand layer was initially above the soft soil layer (Sireesh, Sitharam, and Kumar Dash 2009). Henceforth, whatever load comes over the weak layer will be taken care of by the granular layer and the tensile force generated in the geogrid reinforcement, thereby reducing the overall settlement. Generally, the settlement of the structure laid on soft soil will be high; therefore, settlement predictions should be accurate. The improvement of bearing capacity and settlement of soft soil is mainly due to the three mechanisms: shear layer effect, confinement effect, and additional surcharge effect, respectively, are explained with sketches in Figures 1(a, b, c). The shear layer effect encompasses the shearing resistance offered by a thin layer of cohesionless soil against the superstructure load. The tension generated in the geogrid material will try to confine the dispersing load by counteracting it in the opposite direction, providing a confinement effect. The reason for tensile force in the geogrid is a result of frictional force induced between reinforcement and granular soil. The stress along the punching shear surface acts as an additional surcharge and contributes to bearing capacity improvement. The tensile force generated in each case and the corresponding improvements in bearing capacity was mentioned below in theoretical equation format.

The shearing forces that are developed at the edges of the footing due to the shear layer effect are given by (Jayamohan and Shivashankar 2015)

**CONTACT** Deendayal Rathod deendayal@nitt.edu Department of Civil Engineering, National Institute of Technology (NIT), Tiruchirappalli, Tamil Nadu, India

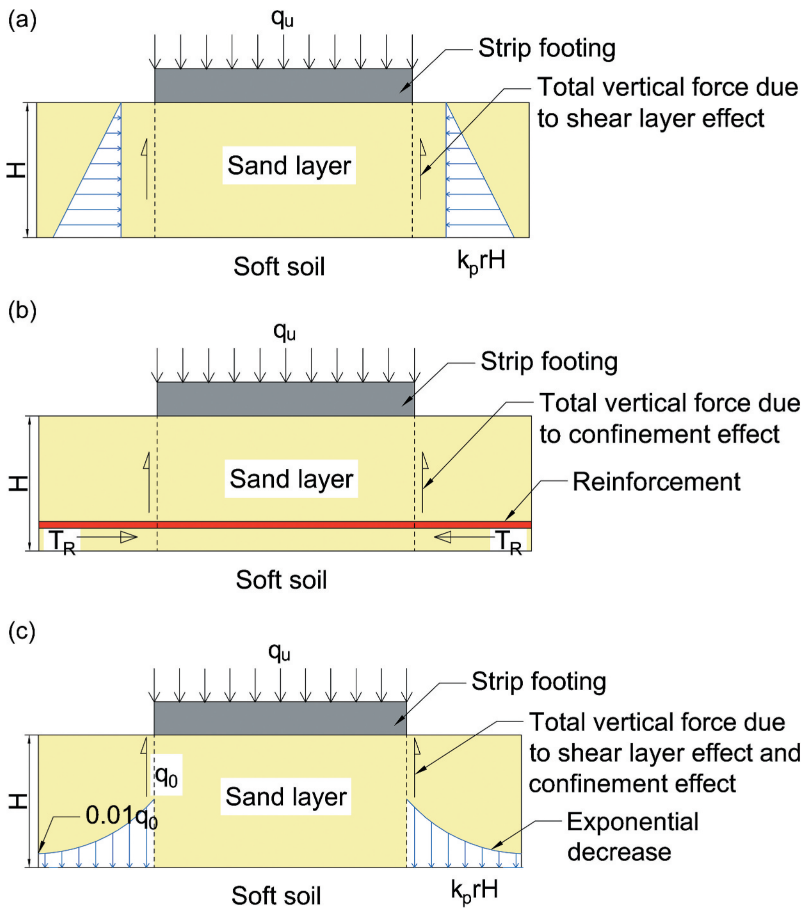


**Figure 1.** (a) Schematic representation of shear layer effect (Adapted from Jayamohan and Shivashankar (2015)). (b) Schematic representation of confinement effect (Adapted from Jayamohan and Shivashankar (2015)). (c) Schematic representation of additional surcharge effect (adapted from Jayamohan and Shivashankar (2015)).

$$\tau_{f1} = \frac{1}{2} K_p \gamma H^2 \tan\emptyset_s \quad (1)$$

The improvement due to the shear layer effect:

$$\Delta Q_{SL} = \frac{2\tau_{f1}}{B} \quad (2)$$

Vertical force in punching shear failure due to the confinement effect is given by Equation (3)

$$\tau_{f2} = T_R \tan\emptyset_s \quad (3)$$

where,

$$T_R = \gamma H \tan\emptyset_R L_e (LDR) \quad (4)$$

The improvement due to confinement effect:

$$\Delta Q_{CE} = \frac{2\tau_{f2}}{B} \quad (5)$$

The improvement due to additional surcharge effect:

$$\Delta Q_{SE} = 0.84(\Delta Q_{CE} + \Delta Q_{SL}) \quad (6)$$

This study provides an overview of geogrid's main applications in geotechnical and related fields. The complex relationship between soil and geosynthetics can be changed by altering the geogrid or the soil's physical characteristics. Even within the same soil, shear stress mobilisation along the geogrid reinforcement direction varies depending on the relative density and level of stress. Under normal load conditions, dense soil has a tendency to dilate. However, the reinforcement prevents this dilation and increases soil–structure interactions, thereby increasing strength. This cutting-edge review aids in comprehending various literature involving interactions of a wide range of geogrid materials (polypropylene, polyethylene, and polyester) with different types of soils ranging from cohesionless to cohesive. The study also highlights the advantages of using tensile materials like geogrids over other options, such as excavation of poorer quality soil and replacement with competent hard soil for pavement foundation, grouting with cement lime for slope stabilisation, installation of piles to increase bearing capacity under footings, and so on. All of the scenarios mentioned above can be remedied using geogrid, which has been demonstrated to be a superior material. It functions as a stress-relieving layer and boosts the soil's bearing capacity (Chakraborty and Kumar 2014; Saha Roy and Deb 2017; Lai, Chen, and Li 2018; Halder and Chakraborty 2018; Xie, Leshchinsky, and Han 2019; Useche-Infante et al.

2022). Another issue that will be addressed in this study is the use of geogrid design shear lag approximation assumption (Abramento and Whittle 1995). Most of the literature exemplifies that the tensile force in a geogrid is distributed uniformly across its width, like loading on a beam. In practice, the tensile force is not distributed uniformly due to soil structure interaction. Understanding the precise tensile force distribution along the width of the geogrid thus requires a thorough understanding of the pull-out response and the generation of interface traction for the exact tensile force distribution along the width of the geogrid (Ragui Wilson-Fahmyfl Robert et al. 2012; lin Wang et al. 2021).

A research gap that needs to be filled for the benefit of practicing engineers is the effectiveness of triangular aperture geogrid and the mechanism of interaction with soil under dynamic loading, especially in pavement foundations (Wang et al. 2018). The durability of geogrid is another issue that is still a problem and should be addressed appropriately. It is necessary to conduct extensive research on the stress relaxation in tensile strength behaviour of geogrid after a specific interval of time because the early age strength of geogrid weakens over time (Jeon 2010; Silva Vieira and Pereira 2021). The vertical reinforcing effect of geogrids, which can provide radial restraint to structures resting on soft soils, has recently received very little literature study. The problem of higher loading will be solved by using a geogrid-encased stone column rather than other geosynthetic materials like geocells. For further stress reduction by the lateral confinement concepts, additional horizontal geogrid reinforcement could be offered in addition to vertical encasing. However, very little research has been done on this subject.

### *1.1. Application of geogrid reinforcement*

The majority of geogrid applications are in pavements, footings, MSE walls, soil slopes, and pile-supported embankments. However, even though geogrid applications in those areas are limited so far, there are certainly other areas where we can use geogrid. This section describes some of them in seismically prone areas, landfill sites, railway ballasts, geosynthetic encasement of stone columns.

Unprecedented earthquakes are not forewarned, even in earthquake-prone regions where large fault movements and plate deformations occur. To mitigate or minimise the catastrophic damage caused by an earthquake, the soil foundation on which the structure is built must be stabilised along with the retrofitting of the structure. Recently, it has been proven that gabion, geogrid, and sheet pile reinforcements ensured resilience against earthquakes, as seen in the study by Chaudhary et al. (2018). However, we are underestimating the actual stresses and deformation in the laboratory. Because in the field, the surcharge load includes hundreds of metres of the soil layer in some instances, which we cannot simulate in our model tests. Centrifuge tests, on the other hand, have the advantage of high-accuracy real-world simulations, even when testing small-scale models under higher gravitational forces (Izawa and Kuwano 2011). These are safer than real field simulations, allowing the researcher to test the behaviour of the structure in a controlled environment.

Ke et al. (2021) conducted a one-year field monitoring of a geogrid-enhanced municipal solid waste landfill. However, the project failed due to the small aperture size, insufficient geogrid length beyond the slip circle, and poor frictional behaviour. Uneven sliding and damping pressures caused inconsistent strains in the reinforcements, which caused instability. These errors can be rectified, and geogrids can be used in landfills in the future. Rajesh and Viswanadham (2012, 2014) used a centrifuge simulation subjected to distortion. The authors observed that the reinforcement effect of the geogrid eliminated the tensile stress and strain generated in the landfill cover. Furthermore, the tension zone's depth was significantly reduced due to the geogrid's improved tensile load strain characteristics. They also demonstrated the significance of using stiffer geogrid subjected to higher levels of overburden stress in order to prevent differential settlement.

Geogrids can also be used in railroads to reduce ballast thickness and prevent aggregate material loss. Various percentages of fine material were used to fill the interstitial voids (fouling) between the ballast (B. Indraratna, Ngo, and Rujikiatkamjorn 2013). The cushioning effect provided by the fouling material and the addition of geogrid between sub-ballast and ballast resulted in reduced displacement. The study also revealed that after a certain level of fouling, the interlocking between the fines and the geogrid diminishes, resulting in excessive deformation. A case study on a geogrid reinforced Shenyang rail line subjected to dynamic loading was investigated (G. Chen 2009). Numerical simulation deduced a conclusion that the propagation of dynamic stress recorded was lesser in the case of a geogrid reinforced rail line.

Geogrid encased stone column is the best reinforcing technique for overhead tank foundations and bridge piers located on poor soils (Zhou and Kong 2019; Yoo and Abbas 2019; Tan et al. 2021; Xu et al. 2021). This most recent topic has concentrated on the macroscopic behaviour of bearing capacity as well as vertical and lateral movements. However, further research is required into the inter-particular interaction between aggregates and geogrids under different types of loading, as well as changes in the molecular-level interaction under undrained conditions.

### 1.1.1. Application in pavements

Flexible pavement contributes to the major application of geogrid reinforcement due to its improvement in trafficability and reduced vertical deformation under moving vehicular load. AASHTO R50 (2017) design guideline is a widely used geosynthetic reinforced pavement foundation design method. The early age tensile strength and the response of the geogrid to the traffic loading was much faster than that of the geotextile, making it a superior material over the geotextile (Nair and Madhavi Latha 2014; Nejad et al. 2016). Moreover, it was found that the positioning of geogrid is the key to getting reliable results. Giroud et al. (2004) reported that using geogrid reduced the base course thickness because the moving traffic load was shared between the base geomaterial and the geogrid, making the subgrade more resistant to deformation. The lateral restrainment and tension membrane affects aid in safe load transfer through reinforcement and controlled strain generation in the system. However, due to overburden pressure and cyclic loading, soil property deterioration was possible as we were dealing with stiff geogrid. This stiff geogrid resisted the compaction process, resulting in a weak interlock between the soil and the geogrid. Therefore, bending stiffness parameter provision could yield a better interlocking properties and safety to pavement foundations. As a result, the consideration of this parameter in the design process could identify promising future research. El Naggar, Turan, and Valsangkar (2015) manifested the beginning of a robust application of geogrids on the safety of underground utilities, such as water and gas transmission pipes, culverts for water passage to nearby irrigation fields, electrical cables buried under the right of a way of highway pavements. Including geogrid reinforced loading platforms reduced the overstressing and excessive deformations transferred onto the culverts, ensuring the safety of underground trenches. As a future likelihood, the moving traffic load simulation in the laboratory is becoming important since our studies were limited to static loading cases. Extrapolating static to real field scenarios will accurately predict the failure stresses and strains on buried utilities.

Work is still being done to simulate the behaviour of pavements under cyclic loading and to develop a design method for determining the base layer thickness reinforced with triangular geogrids Qian et al. (2013). The authors studied three cases without a geogrid, with a weaker geogrid (TX1), and with a strong geogrid (TX2). Results showed that providing triangular geogrid at the interface between the base and weak subgrade layers decreased the maximum vertical stress and permanent deformation under repeated cyclic loading. The stress and deformation variation with the load cycles are represented in Figure 2(a, b). The benefits of geogrid reinforcement could be quantified in terms of resilient modulus increment or base thickness

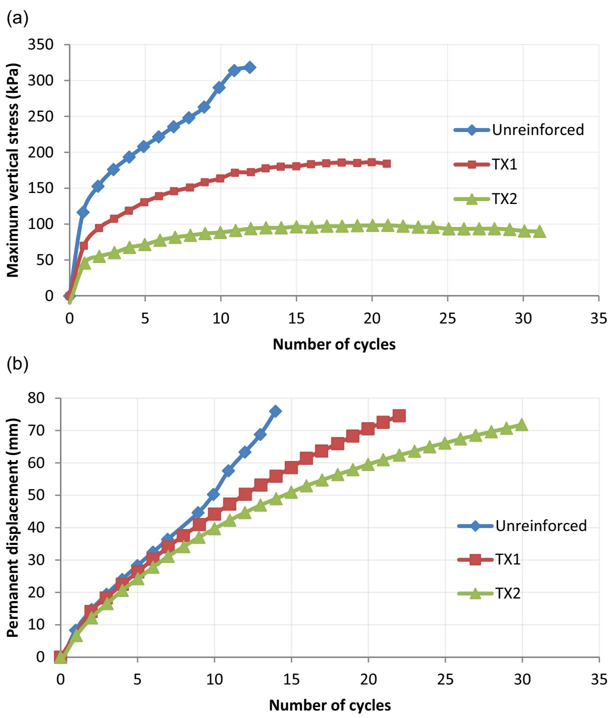


**Figure 2.** (a) Vertical stress distribution at the base–subgrade interface (adapted from Qian et al. (2010)). (b) Permanent displacement at the surface versus the number of load cycles (adapted from Qian et al. (2010)).

reduction. The resilient modulus is the slope of the unloading curve for any particular loading cycle, and it also includes elastic strain and relaxation. Nonetheless, rigid plates of moderate dimensions were used for cyclic loading applications. However, in the actual scenario, the single axle load of 80kN was acting as a point load, and authors simulated it as a surface loading on purpose for most of the study (Qian et al. 2013; Ravi et al. 2014; Nair and Madhavi Latha 2014; Abu-Farsakh et al. 2016; Jayalath et al. 2021; Abdollahi, Moghaddas Tafreshi, and Leshchinsky 2021). Compared to the pavement surface layer area, the contact area of axle loading is negligible, so we could assume it is almost as a point load. This misinterpretation of loading should be avoided in the forthcoming studies for an exact portrayal of the results.

Until now, this study discussed the flexible pavement reinforced with geogrid. The usability of geogrid is not limited to flexible pavements. Pavement overlay can be of concrete or asphalt, depending on the feasibility and purpose to serve. The incorporation of geogrid to reinforce plain cement concrete has gained attention. We know that concrete is good at compressive load but has poor tension capacity. Geogrid, a tensile material, can be beneficial in strengthening plain cement concrete (PCC) and will give imminent warning before failure. The ductile post-cracking behaviour in the geogrid reinforced plain concrete rigid pavement increased load-carrying capacity and decreased crack propagation Al Basiouni et al. (2018a). Al-Hedad, Zhang, and Hadi (2020) presented works showing that concrete pavement reinforced with geogrid reduced the shrinkage in pavements due to temperature fluctuations. Draining out of the water from the concrete pavement where the water table is shallow leads to corrosion of steel reinforcement and other conventional materials, but geogrid replacement avoids the formation and propagation of cracks and corrosion. Other significant findings on geogrid-reinforced pavement foundations and parameters are studied and compiled in Table 1.

#### 1.1.2. Application in footings

Over the years, numerous works have been successfully performed to explore the usage and outcomes of geogrid reinforced footing load. Several laboratory tests, numerical modelling, and simulation studies are available in the literature, whereas field studies are limited. In particular, the critical parameters, which directly affect the performance of reinforced footing beds and thereby aid in attaining maximum bearing capacity are the burial depth of placement of the top geogrid layer, the number of reinforcement layers, diameter, and aperture geometry, and so on. For the burial depth of geosynthetics, Aria, Kumar Shukla, and Mohyeddin (2020) used finite element analysis using PLAXIS software under plane strain conditions to determine the bearing capacity change due to the variation in depth of placement of geogrid and the width of reinforcing element. The behaviour of the foundation soil was simulated using the Mohr–Coulomb elastoplastic constitutive model. This most basic constitutive relation assumes that the soil exhibits elastic behaviour before failure and a sudden shift to perfectly plastic as failure occurs under shifting stress states. For the entire study, loose sand was used. The Mohr–Coulomb approximation is sufficient for loose sand with an extended elastic range or elasticity. The optimum burial depth of reinforcement under the footing was said to be dependent not only on the footing width but also influenced by soil shear strength parameters like cohesion and angle of internal friction. Most of the past literature has not addressed the reason for shear parameters' dependence on the reinforcement's burial depth.

The Soil-Geogrid interaction study is another area of prime importance, as the interlocking between the soil and geogrid shows the effectiveness of reducing the load transferred to the strata beneath the geosynthetic layer. Under various loading conditions, the ASTM D5321 standard test method provides a way to measure the interfacial friction between the footing and the geogrid. This can be quantified in terms of interface strength parameters with a model pull-out testing set-up. In the recent past, complex soil–geosynthetics interaction studies have been carried out to capture the actual failure pattern during foundation loading. Chen et al. (2021) studied the behaviour of sand under strip footing with and without geogrid inclusions. Due to the opacity of sand, transparent-type sand was used to understand the displacement along with the different layers of geogrid, failure behaviour, and so on. The results revealed that the number and length of reinforcements were the key parameters. The failure trend seen in the geogrid reinforcement commences from the bottom layer and is then directed towards the surficial layers. (Chung and Cascante 2007) also concluded the importance of parameters like the number and location of reinforcement in improving the bearing capacity as well as the small strain stiffness of underlying soil owing to the benefit of dispersing action of reinforcement to distribute the load to a deeper layer where the strength, confinement, and stiffness were predominant. (Michael, By, and Collin 1997) studied the effect of soil density and the reinforcement plan area beside the above-mentioned parameters. This paper shows a top reinforcement layer close to the surface added to the bearing capacity enhancement. Even though the author's paper was case-specific and used only a certain type of soil with varying densities and a particular type of

**Table 1.** A summary of the the literature on geosynthetic-reinforced pavement foundation.

| References | Reinforcement type | Geogrid location | Tank dimension/ specimen dimension | Asphalt (HMA) thickness | Base thickness | Subgrade thickness | Parameters studied | Significant findings |
|---|---|---|---|---|---|---|---|---|
| Qian et al. (2013) | Triangular aperture geogrid | At the interface of base and subgrade | 2 m×2.2mx 2 m | - | 150 mm, 230 mm, 300 mm | 1000 mm | Base thickness<br>Permanent displacement<br>Max. Vertical stress at the centre | Geogrid reduced the maximum vertical stress on subgrade<br>Confinement provided by aggregate-geogrid interlocking was key to reinforcing the base course |
| (Al Basiouni et al. 2018b) | Biaxial geogrid | In Portland, cement concrete | - | 170 mm | 280 mm | 600 mm | Load capacity and Crack propagation of geosynthetic reinforced concrete (GRC) | GRC improved post-cracking ductility of GRC compared to PCC<br>Steel and geogrid exhibited similar behaviour<br>GRC sustained three times more load cycles than PCC by reducing accumulated horizontal tensile strains |
| (J. Qian et al. 2018) | Glass fibre geogrid, geotextile | Wearing course | 0.3 m×0.18 m×0.3 m | - | - | - | Crack opening width<br>Traffic load<br>Thermal load | Crack in pavement increased as thermal load increased<br>Placing of geotextile and geogrid retard fatigue and propagation of the crack |
| Correia et al. (2018) | Geogrid | Wearing course | - | 60 mm | 200 mm | 1000 mm | Geogrid strain<br>Max. Rutting depth | Geogrid reduced permanent displacement and strain and mobilised tension in pavement structural layers<br>Increased bearing capacity even for weaker subgrade |
| (B. Han et al. 2018) | Biaxial and triangular geogrid | Between aggregate base | 0.5 m×0.5 m×0.18 m | - | 360 | - | Shear displacement<br>Geogrid-soil interaction in terms of resilient interface shear modulus ($G_i$) | By increasing cyclic shear stress, the interface shear modulus decreased<br>By increasing normal stress, $G_i$ increased under cyclic shear testing |
| (Robinson et al. 2020) | Biaxial and triangular geogrid | Base/ subgrade interface<br>Mid depth base | 58 m×11mx1.1 mm | 107 mm | 362 | - | Rutting performance<br>Subgrade pressure | The preferred location of geogrid is at the base/ subgrade<br>Increasing aperture size and tensile strength improved rutting performance |
| (B. Han et al. 2020) | Biaxial and triangular geogrid | Between aggregate base | 0.533 m×0.38 m×0.115 m | - | - | - | Aggregate gradation<br>Geogrid tensile strength and aperture geometry | A better reinforcement effect was obtained by increasing aggregate interaction with geogrid<br>Aperture geometry is inferior compared to tensile strength on reinforcing effect<br>Triangular geogrid better than biaxial geogrid |
| (Alimohammadi et al. 2021) | Triaxial geogrid | Base/ subgrade interface | - | - | 152 mm | - | Geogrid stiffness<br>Geogrid location<br>Asphalt and base layer thickness | The project cost was reduced by reducing the asphalt and aggregate base thickness through the incorporation of geogrid<br>Geogrid reduced vertical stress at the top of the subgrade due to its lateral confinement effect |

geosynthetic reinforcement, still the bulk of the innovations was based on the basic knowledge provided by this classic paper.

In seismic-prone areas, providing a thin sand layer and reinforcement of the shallower depth with optimum width will significantly reduce the damage to weak soil mass and foundation subjected to a seismic acceleration in the horizontal and vertical directions. Kumar and Chakraborty (2020) analysed the bearing capacity improvement for a strip footing resting on a geogrid-reinforced sand bed subjected to pseudo-static seismic loading using a lower bound limit equilibrium theorem and finite element analysis. Despite the tremendous enhancement in load-carrying capacity evident from the study, the results were not accurate. Because they did not use time, frequency, and vibrational shear waves transmitted through the soil for their dynamic analysis. This study could be further modified by incorporating dynamically prominent parameters for a better approximation of dynamic loading conditions. Another problem we intervene in dealing with footing is the interference effect on closely spaced footings. We are forced to design a large footing to cope with the heavy superstructure loads, which will result in a reduction in the spacing between footings. (Saha and Deb 2019) investigated the interference effects of footing resting on geosynthetic reinforced granular soil underlain by soft soil. The schematic set-up of footing resting on a geogrid reinforced sand layer underlain by weak soil is illustrated in Figure 3(a,b) Initially, the bearing capacity showed an increase, then reduced with the increase in spacing. To alleviate such problems, optimum spacing between reinforcing members was provided. The author also studied the effects of different footing geometry. Square footing showed an increased bearing capacity than that on rectangular footing. However, significantly fewer studies were conducted on the geogrid reinforced ring or circular-shaped footings. Even though ring foundations have a wide range of applications in bridge piers, overhead tanks, silos, cooling towers, and so on, the study was limited. Efforts to conduct studies to stabilise the excessive load transferred to ring footings will reduce the ambiguities prevailing in these fields. Table 2 shows the important parameters affecting the load-carrying capacity of the geogrid reinforced footing base and its optimum value chosen by the authors.

### *1.1.3. Application in MSE walls*

Mechanically stabilised earth walls consist of facing blocks, backfill soil, and reinforcing materials. The choice of material is based on the purpose to be served. The facing panel helps to avoid the ravelling of soil,

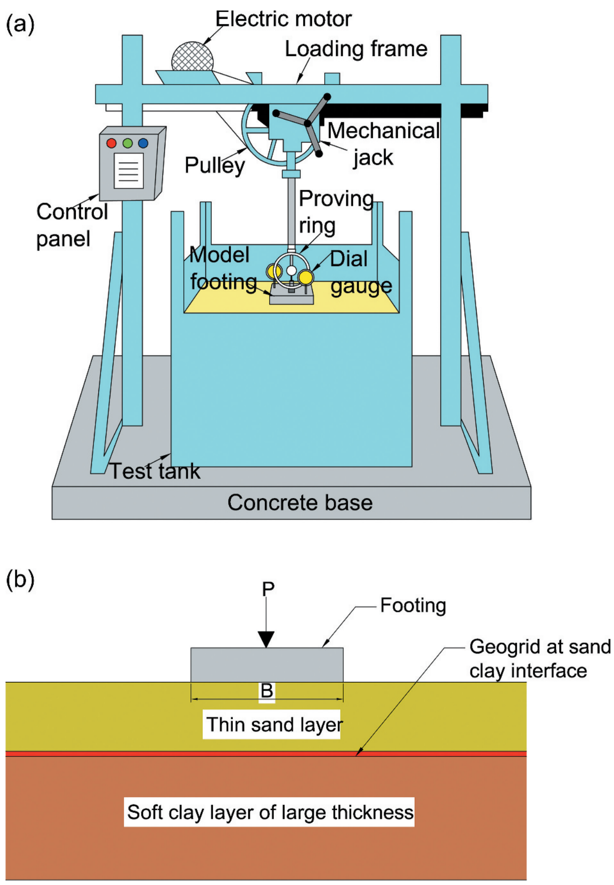


**Figure 3.** (a) Schematic diagram of test set-up for isolated footing (adapted from Saha and Deb (2020)). (b) Schematic diagram of footing on a reinforced bed (adapted from Saha and Deb (2020)).

**Table 2.** Optimum parameters of geogrids used in the previous studies.

| Researcher | Type of footing | Type of reinforcement | h/B | u/B | b/B | N |
|---|---|---|---|---|---|---|
| Chen et al. (2021) | Strip | Biaxial polypropylene geogrid | 0.25 | 2 | >3 up to 7 | 6 |
| Hosamo et al.(2021) | Ring | Single and double-layered biaxial geogrid | 0.15 | 0.4–0.45 | - | 4 |
| Saha and Deb (2020) | Isolated Square footing | Geogrid | 2 | 0.75 | - | - |
| Khosrojerdi et al. (2019) | Square footing | Geogrid | 0.3 | 0.3 | 1.5 | 3 |
| Xie et al.(2019) | Strip footing | Geogrid | 0.5 | - | 4 | - |
| A. Kumar and Saran (2003) | Strip and square | Tensar geogrid | 0.5 | 0.25 | 6 | 2 |
| Halder and Chakraborty (2018) | Strip footing | Geogrid | 0 | 0.5 | 4 | - |
| Yadu and Tripathi (2014) | Strip footing | Biaxial geogrid | 0.33 | 0.33 | 12 | 6 |
| Boushehrian and Hataf (2003) | Circular footing | Geogrid | 0.33 | 0.56 | - | 3 |
| (Adams and Collin 1997) | Square | Biaxial geogrid & geocell | 0.16 | 0.25 | - | 3 |
| Khosrojerdi et al. (2019) | Square footing | Geogrid | 0.3 | 0.9 | - | 3 |
| Halder and Chakraborty(2019) | Strip footing | Planar geogrid | 0.45 | 0.3 | 5.5 | 2 |
| Sawwaf and Nazir (2010) | Rectangular footing | Geogrid | 0.6 | 0.3 | 5 | 3 |
| Zidan (2012) | Circular footing | Geogrid | 0.2 | 0.19 | - | 4 |

and it can be of concrete, timber, gravel, and so on. Reinforcing elements like steel strips or geogrid sheets provide sufficient tensile strength, stiffness, durability, and pull-out strength, which helps the designers to reach extreme wall height irrespective of the gravity load and slope angle (ASTM 1995). There are two types of design aspects of the reinforced MSE walls. These are the tie-back wedge method and the coherent-gravity method, as illustrated in Figure 4 (a, b). Tie represents a tension member, and it is driven into the active failure zone of the soil. The tie member will stabilise the active failure wedge. Failing wedge boundaries could be located using monitoring devices like earth pressure cells and strain gauges along the entire reinforcement length. As friction develops along with reinforcement, strain mobilisation will occur, and all failed wedge boundaries can be plotted using FLAC 3D or PLAXIS 3D software. Increasing the height of an unreinforced MSE wall requires increased horizontal space, which is difficult to afford in applications like highway embankments. This space consumes the right of way for the pavements. Therefore, a geogrid in the form of steel strips was introduced in a layered manner with one end tied to the wall facing element. The tension membrane effect provided sufficient lateral resistance against soil movement. A secondary reinforcement layer of a shorter length could be a wise choice to reduce the overall cost of the improvement Jiang et al. (2016).

Fishman et al. (1993) conducted an experimental study on a full-scale concrete facing a mechanically stabilised tensor geogrid reinforced earth retaining wall that was used as part of a highway widening project. Internal and external stability must be considered when designing a retaining wall. Exterior walls ensured the external stability of the system. The external instability issues observed were sliding failure, overturning failure, tilting/bearing failure, and slip failure. However, the author only looked at the internal stresses and strains within the system. The internal failure modes in the design of reinforced soil retaining walls were tension failure and pull-out failure. The study revealed that the tensile strength and stiffness of the reinforcing member should be adequate to prevent the breakage of the tensile member. Moreover, pull-out failure could be eliminated by providing a sufficient length of the reinforcing members beyond the potential failure wedge. The observed vertical pressure induced near the wall facing was a smaller value than that at the centre and the other end of the retaining wall. This was due to the soil-arching effect observed near the wall face and the temperature stresses generated. This effect could be minimised by using a flexible articulated panel instead of a rigid concrete retaining wall.

The performance of multiple tiered stepped facing MSE wall reinforced with geogrids subjected to strong ground motion is becoming relevant nowadays. A recent number of papers in that particular area show its importance (Xiao et al. 2012; Safaee, Mahboubi, and Noorzad 2021). A shake table test was used to simulate ground shaking. The number of steps for the concrete fascia and the closely spaced reinforcement layers positively affected the system's internal stability. The geogrid members reduce the earth pressure generated from the ground shaking by evenly distributing the pressure across the MSE wall, thereby avoiding potential pockets of failure points. Moreover, the drainage properties of the geogrid prevented the accumulation of excessive pore water pressure and thereby contained the threat of liquefaction-induced damages to wall-facing and backfill soils. The geogrid reinforcement also eliminated the displacement and overturning effects under high-intensity ground shaking Qu et al. (2022).

The same principle applies to bridge abutments and approach backfill. Gregory et al. (1993) conducted a two-parameter finite element study on bridge abutments. The study interpreted that geogrid introduction into the backfill reduced the permanent settlement and differential settlement, resulting in a bump at the ends of the bridge. A collapsible material was positioned between the fill and the abutment to reduce the earth pressure exerted on the abutments. Thus, the result of the study concluded that the tensile reinforcement and the collapsible inclusions reduced the settlement and thereby ensured the satisfactory

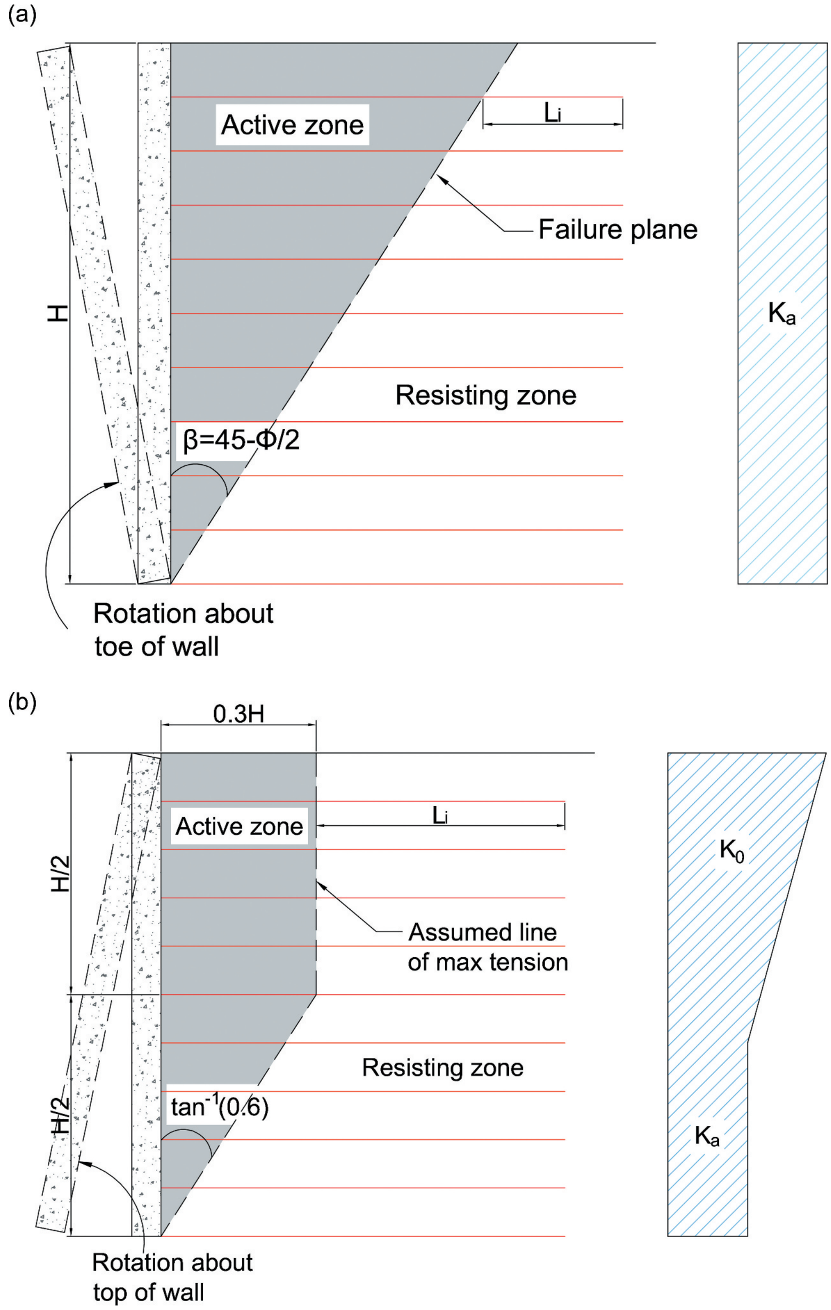


**Figure 4.** (a) Schematic representation of tie-back wedge method (adapted from Molly and Katti (2014)). (b) Schematic representation of coherent gravity method (adapted from Molly and Katti (2014)).

performance of the bridge system Zhang, Zheng, and Lu (2014). A parametric study by varying collapsible layer thickness, stiffness of collapsible and reinforcing materials, and so on should be conducted to better understand the importance of these cushioning layers. A shake table test investigated the dynamic response of a geosynthetic reinforced soil (GRS) abutment Zheng et al. (2018). The schematic view of the GRS abutment system supporting the bridge beam and overlying pavement is shown in Figure 5. The results showed that under the influence of earthquake motion, the geogrid reinforced abutment and modular facing blocks underwent less deformation. The addition of lateral and longitudinal reinforcement could increase the potential height restriction of the bridge abutment. All of the significant critically analysed findings related to the geogrid-reinforced MSE wall have been documented in Table 3.

#### 1.1.4. Application in reinforced soil slope

Reinforced soil slopes enable us to provide steep slopes with limited usable space. This talismanic technique is designed with the aid of the limit equilibrium method or design earth pressure coefficient approach (Park et al. 2007; Halder and Chakraborty 2018, 2019). The driving moment caused due to the weight of the sliding soil mass and its eccentric loading leads to the formation of a slip cycle along

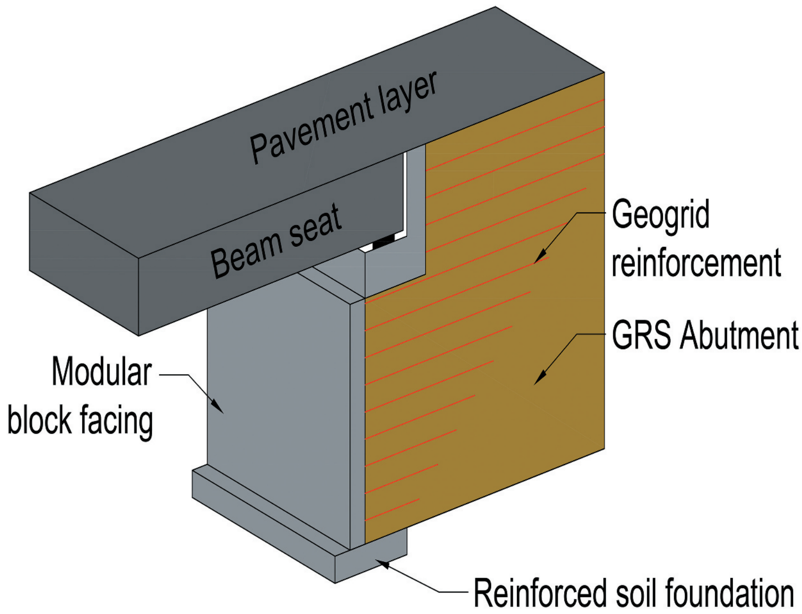


**Figure 5.** Geogrid reinforced soil (GRS) bridge abutment.

the slope. The provision of stiff reinforcement at an appropriate location crossing the failure slip line provides an additional resisting moment, thereby making the system stable. Figures 6(a, b) show the relationship between the geogrid's tensile strength and the separation between the centre of rotation and the axial direction of the force that adds to the resisting moment. Limit equilibrium simplifies the geometry and loading conditions by assuming that the slope is in equilibrium at failure. It cannot, however, capture the complex nonlinear behaviour and strain softening. However, most of these factors, as well as various failure modes, are considered by finite element methods (Fawaz 2014; Ayob et al. 2019). In the analysis and design of the embankment, we need to corroborate the rotational stability, lateral sliding stability, and extrusion stability to achieve adequate safety factors. A pictorial representation of the reinforcing mechanism in the embankment soil slope is illustrated in Figures 7(a, b, c). In rotational-type failure, one component of tensile force interacts with and acts against the driving force. One form of analysis is simplified Bishop's method, in which we divide soil mass into vertical slices and analyse. The geogrid incorporation of the soil mass will add to the resistance force to keep the wedge in equilibrium and thereby yield an improved overall safety factor. The lateral spreading type of failure is prevented by restricting the horizontal movement of soil fill by the tensile force generated in the reinforcement, which acts in the opposite direction. Foundation extrusion is the horizontal movement of the foundation material (not the fill movement) due to differential settlement, inappropriate design, and soil instability (Romeo, Pezzano, and Rimoldi 2022). The solution to this mode of failure was to reduce the settlement by making the embankment base stiffer.

Fahel et al. (2000) presented a field study of reinforced bridge abutment highways in Brazil. The embankment fill consisted of sand, and the foundation soil was soft. Soft soil has low shear strength and permeability, making them a poor choice of construction. Therefore, a stability analysis was mandatory to ensure the safety of existing structures, settlement, and lateral deformation of the embankment. The geogrid reinforced embankments were more stable due to their confinement and separation functions, thereby permitting controlled construction. Due to the poor consolidation rate of soft clayey deposits and our preference for stepped construction, the rate of consolidation was relatively slow in the study area. Synthetic vertical drains were provided along with geogrid to accelerate the consolidation process and to reduce consolidation-related settlements (Rowe and Li 2005). The provision of stiffer geogrid reinforcement leads to the reduction of horizontal movement of the soil wedge. The horizontal movement (lateral spreading) of soil mass due to the high lateral earth pressure from the embankment and traffic loading was reduced using geogrid reinforcement. This was attributed to the tensile force component acting opposite to the soil driving force. Bishop's method of slices was adopted to analyse the stability of the embankment fill. The study demonstrated that incorporating reinforcement increased the embankment system's safety by preventing rotational failure and lateral sliding of soil mass.

Xu et al. (2019) investigated the failure mechanism of an 8-m-high embankment reinforced with a geogrid. The study outcome illustrated that the reinforcement was strong enough to mobilise the maximum tensile strain due to the surcharge loadings on

**Table 3.** A summary of past works in the literature on MSE wall.

| References | Wall type | Wall height | Reinforcement type | Backfill type | Monitoring instruments | Type of testing | Parameter studied |
|---|---|---|---|---|---|---|---|
| Fishman et al. (1993) | Precast concrete wall | 4.72 m (15.5 ft) | Geogrid | Cohesionless | Resistance strain gauge & inductance coil | Experimental | Geogrid strain, lateral earth pressure |
| Bathurst et al. (2019) | Battered wall | - | Polymeric geogrid | Cohesionless | - | Reliability-based probabilistic approach | Reinforcement length, reinforcement strain |
| See Keung Ho and Kerry Rowe(1994) | Cruciform aluminium panelled MSE wall | 508 mm (20in) | Geogrid geotextile | Sand | Strain gauges, 2 LVDTs, pressure cells | Plane strain Finite element method (1 g-12 g)- AFENA Centrifuge modelling | Interface shear strength between fill and reinforcement, lateral earth pressure, vertical pressure |
| Mane and Viswanadham (2012) | Perspex sheet faced-wall | 270 mm | Geogrid geotextile | Dry sand | Permanent L shaped markers for strain measurement, LVDT | Centrifuge modelling FEA-PLAXIS 2D (10 g-75 g) | Wall inclination, vertical spacing, crest settlement |
| Saran et al.(1992) | Mild steel MSE wall | 8 m | Aluminum bamboo | Dry sand fill | - | Theoretical analysis-Limit equilibrium approach-Model experiment | Lateral earth pressure, reinforcement length, surcharge loading, rotation of the wall |
| Gregory Monley et al. (1993) | Rigid abutment wall | 3.6 m | Geogrid Nonwoven geotextile | Granular fill | Deformation gauge, strain gauge, earth pressure gauge, tension gauge | Field test & FEA | The axial stiffness of reinforcement, surcharge loading, settlement |
| Zhang, Zheng, and Lu (2014) | Bridge abutment wall | 5 m | Geogrid | Sand | Earth pressure cell, settlement gauge | Numerical analysis – PLAXIS | Lateral displacement, maximum settlement, tensile stiffness of geogrid |
| Zhang et al. (2007) | Bridge abutment wall | 2.16 m | Stiff polymeric geogrid | Silty sand Sandy silt Silty clay | - | Theoretical analysis- 2D Limit equilibrium approach-PCStabl 6 Numerical analysis-FLAC 3D | The vertical settlement, lateral movement, loading rate |
| Juran and Chen (1989) | Earth wall | 13 m | Aluminum strip reinforcement | Cohesive | Earth pressure cell, settlement gauge | Limit stress analysis & Numerical Full-scale experiments Reduced scale model tests | Loading, lateral displacement, maximum settlement, tensile stiffness of geogrid |
| Sridharan et al. (1991) | Earth wall | - | Tor steel (cold twisted, deformed bars) Mild steel bars Mild steel flats | Cohesive | Tension-proving ring, self-straining loading frame | Experimental | Sand layer thickness, pull-out length |
| Bozorgzadeh et al.(2020) | Steel strip MSE wall | 16.9 m | Steel strips | Cohesionless frictional | - | Reliability-based probabilistic approach | Spacing, probability of geogrid failure, equivalent surcharge height, depth |
| Dennes Bergado et al. (1992) | Earth wall | 5.7 m (18.7 ft) | Steel grid galvanized steel wire mesh reinforcement | Weathered clay Clayey sand | Strain gauge, Pneumatic piezometers, earth pressure cells, inclinometers | Laboratory test Field pull-out test | Overburden pressure, backfill material, axial strains |

the fill. Moreover, the formation of the slip surface was formed well inside the soil mass and thus alleviated the threat of slope failure. Fast Lagrangian analysis of continua (FLAC 3D) helped identify the mode of failure assumed to be happening in the field. Even at present, the actual failure mechanism of the reinforced slope is still a mystery. The authors showed some insights into the failure mechanism of an 8-m-high embankment. Real-time monitoring devices were attached to quantify the vertical stress, settlement, and so on, over time to better understand failure mechanisms.

An extensive study involving six possible failure modes and five associated types of slip lines was elaborately investigated by Lai, Chen, and Li (2018) using PLAXIS 2D. Trapdoor failure mode was seen for shallower voids whose failure surface starts from the embankment top to the top of the void ($m < 0.1$, $n < 0.5$). Sidewall failure was seen for deeper voids ($m > 0.1$, $n < 0.5$), and the failure was

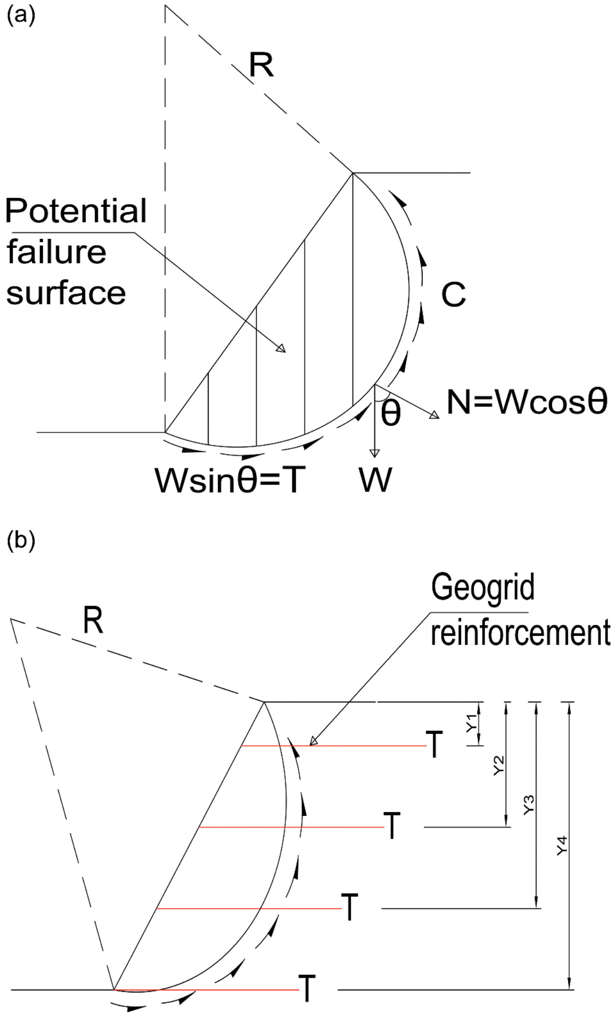


**Figure 6.** Unreinforced soil slope. (b) Geogrid reinforced soil slope.

mainly due to increased lateral earth pressure. Rotational failure was observed due to the nonlinear load on the overlying void and the orientation of slip lines towards the larger load. Void eccentricity created the lateral sliding failure. Combined failure was the last failure mode observed in the numerical study, and it was developed due to the thinner roof of the void. The selection of geogrids in the study was based on the location of the void below the embankment (i.e., *m* value). The schematic diagram of the embankment overlying a void is delineated in Figure 8.

#### *1.1.5. Application in geosynthetic-reinforced pile-supported embankment*

A combination of pile and geogrid support is necessary to alleviate the differential settlement and horizontal displacement between existing and proposed pavements. Zhao et al. (2019) conducted a coherence study on geogrid reinforced pile-supported highway embankments as a part of a highway widening in China. The project involved different soil terrains, including soft compressible, or expansive soils. The soft soil was overlain by a thin layer of aggregate placed along the basal embankment width, and geogrid was installed in succession over the fill area. Inclinometers at 22.5 m were installed to quantify the horizontal deformation. Furthermore, a settlement tube with several strain gauges was buried in the soil to examine the settlement of each layer of reinforcement. The tension membrane effect of the reinforcing member and

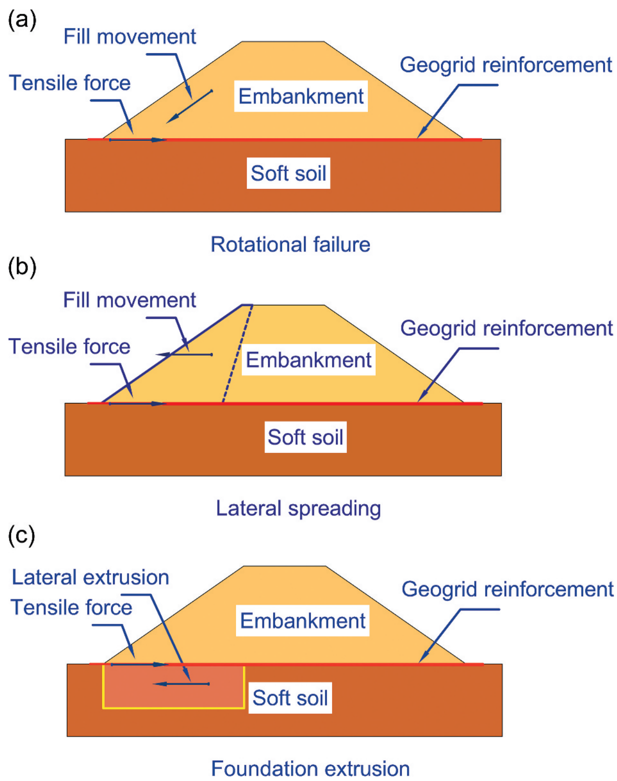


**Figure 7.** (a) Base reinforcement mechanism - rotational failure (adapted from 2020)). (b) Base reinforcement mechanism - lateral spreading (adapted from 2020)). (c) Base reinforcement mechanism - foundation extrusion (adapted from 2020)).

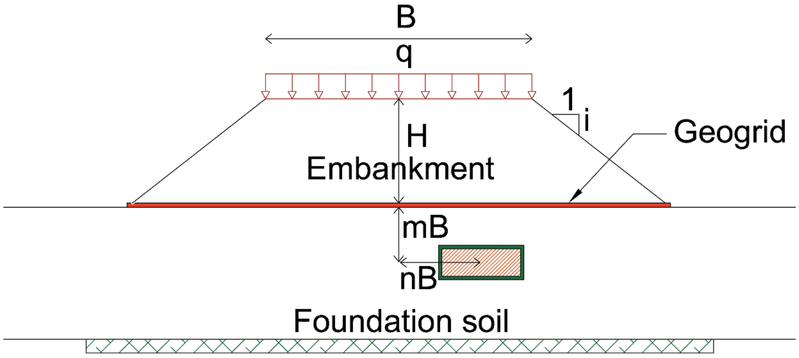


**Figure 8.** Geosynthetic-reinforced embankment overlying voids (adapted from Lai, Chen, and Li (2018)).

the passive soil arching effect achieved the settlement reduction. A conventional pile-supported embankment requires heavy piles to be placed at frequent intervals. However, the advent of geogrid incorporation in piled embankments reduced the cost of construction materials by reducing the number of piles required Liu et al. (2007). Earlier, soil arching was the only mechanism opposing the load. The tension membrane effect is now added to counteract against the load imposed.

Several authors studied the mechanism of soil arching experimentally and numerically (Zhuang and Cui 2016; Zhuang and Wang 2018). Soil arching is the downhill movement of soil resulting in upward shear resistance opposing the load acting on the embankment as illustrated in Figure 9. This effect is visible mainly due to the stiffness difference and relative compressibility and differential settlement between the installed pile and the native soil. These two properties, tension membrane effect, and soil arching, respectively, are added to the load-carrying capacity of the embankment. The stress concentration will be more at the high stiff piles and geogrids. Therefore, a transfer of load from soil to pile and geogrid makes the soil-structure system stable by mobilising the shear stress along the length of pile and geogrid (Zhuang and Ellis 2016; Briançon and Simon 2017 Zhao et al. 2019). Recently, this multi-dimensional load transfer mechanism of reinforcing material under the effect of dynamic loading was also investigated (Wang and Chen 2019). However, those studies are pretty complex, and researchers were invited to present simple design approaches to identify these mechanisms as mentioned above in the column-supported embankment system BS 8006 (2010). A similar real field study was conducted by (Han and Akins 2002) to analyse the load transfer mechanism in pile-supported reinforced embankments. To increase the reinforced concrete pile spacing, they introduced four layers of geogrid reinforcement as a part of the entire project cost reduction. Moreover, the geogrid layer transferred the load to the pile, thereby ensuring the system's stability. In addition, the authors used an alternative technique to reduce the cost of highway embankment projects. They replaced piles with a Vibro-concrete column with an enlarged base and compared the results of differential settlement using Vibro-concrete columns and cast in situ columns. However, geogrid reinforced pile embankment was observed to be superior to the vibro-concrete column.

Indraratna, Balasubramaniam, and Balachandran (1992) constructed a trial embankment on soft clayey soil and loaded it up to failure. The failure by rotational instability was quantified using the inclinometers. The critical state finite element program (CRISP) used the field measurement data to conduct a drained, undrained, and consolidated coupled analysis. The associated analysis has given better insights into the actual field partial drainage conditions predominantly seen at a shallower depth. The modified

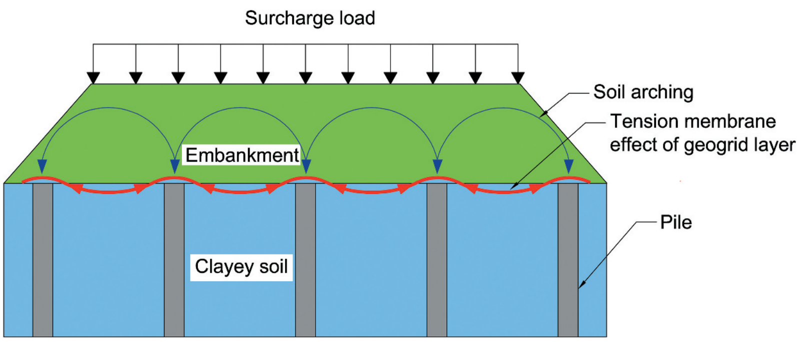


**Figure 9.** Soil arching on geogrid reinforced piled embankment (adapted from Eskişar, Otani, and Hironaka (2012)).

cam clay model used in this finite element program overestimated the settlement value at deeper depths. Furthermore, the high tensile reinforcement addition alleviated the internal tension failure and thereby aided us in providing greater fill height. From the study, it can be envisaged that the reinforcement provision throughout the fill height with optimum spacing would have prevented the vertical tension crack development. Samadhiya et al. (2009) investigated the impact of a geogrid-reinforced granular pile. Direct installation of geogrid in soft clay will not result in bearing capacity enhancement due to the lack of angle of internal friction. As a result, a vertical granular pile arrangement was created, and the geogrid was aligned horizontally inside the granular pile. Furthermore, the authors discovered that providing optimal spacing between geogrid layers and pile reinforcement depth minimised pile bulging, enhanced load-carrying capability, and reduced settlement (Pham and Dias 2021).

## 2. Conclusions

- The geogrid in pavement contributed to the 70–80% utilisation of total geogrid available in the market. The geogrid's reinforcing, separation, and confining properties increased the soil's resilient modulus, load-bearing ability, and pull-out strength. More research has recently focused on comprehending the stiffened platform (tension membrane) effect of geogrid and stress concentration due to stiffness difference between pavement foundation and geogrid under wheel loading to lengthen the pavement lifespan.
- The typical reflection cracking and rutting failures seen in the pavement foundations were eliminated with the incorporation of geogrid at the optimal locations. Moreover, the reduction of base layer thickness was another attribute seen in most studies dealing with the geogrid reinforced pavement.
- The scope of many earlier studies was restricted to flexible geogrid pavements. There is little information available about how well geogrid-reinforced concrete pavement performs. Experiments on geogrid-reinforced Portland cement concrete are essential to improve post-cracking behaviour. In terms of adding tensile strength and preventing corrosion, geogrid is just as effective as steel reinforcement.
- The vertical reinforcing effect of geogrid successfully increased the bearing capacity of weaker soil. Building foundations, bridges, and other structures resting on unfavourable soil could be supported by a geo-synthetically encased stone column, in which geogrid was wrapped around the aggregate column's circumference.
- Numerous carefully scrutinised experimental studies on geosynthetic reinforced footings have shown that bearing capacity and settlement improved with the proper placement, spacing, and number of the geosynthetic reinforcement. Further research is required, however, on the footing close to a reinforced soil slope's edge.
- Pull-out resistance and tensile strength were the two most important factors contributing to geogrid's maximum reinforcing effect. The soil–geogrid interface's traction mobilised higher tension and resulted in lesser stress for higher pullout resistance and tensile strength.
- Geosynthetic reinforced mechanically stabilised earth walls improved the internal stability and shear strength of soil mass owing to geogrid's sufficient pull-out length and tensile strength.
- In bridge engineering, reinforced abutments were constructed using the same reinforced MSE wall principle. Providing a shock-absorbing (geogrid lining) that could decouple the backfill soil and wall facing subjected to seismic acceleration and/or geogrid encased pile supporting embankment kept the bridge system intact. Otherwise, the system would have failed due to differential settlement between the embankment fill and the approach slab.
- Due to soil arching and the tension membrane effect, the permanent deformations in the geosynthetic reinforced pile-supported embankment were lessened. The two mechanisms opposing the load direction increased the safety factor. Greater embankment height was achieved by combining geogrid and pile with these tension membranes and arching mechanisms.
- This study presented the recent advancements in geogrid, including the various failure mechanisms in soil reinforced with geogrid. Moreover, the results of the finite element constitutive modelling and analysis were used to illustrate the mechanism of the complex soil structure interactions. The finite element analysis captured the precise mechanism of soil structure interaction under various stress states.
- Few researchers have measured the deterioration of early-age tensile strength over time, despite the importance of geogrid durability. However, no experimental study has focused on this durability issue. A new technique of prestressing concept could be applied for the loss of long-term tensile strength after a thorough review of the currently available literature. Prestressing, which involves exerting force on a geogrid before embedding it in soil, helps distribute the load evenly across the width. This increases the stiffness and strength of the

geogrid, creating a high-tension membrane effect that increases the bearing capacity by a factor of several.

## Notations

| | |
|---|---|
| h | Vertical spacing between reinforcement layers |
| H | Thickness of granular layer |
| B | Width of footing |
| u | Depth of the first layer of reinforcement |
| b | Length of reinforcement |
| N | Number of reinforcing layers |
| J | Geogrid stiffness |
| $K_a$ | Active earth pressure coefficient |
| $K_p$ | Passive earth pressure coefficient |
| $K_0$ | At rest earth pressure coefficient |
| $\tau_{f1}$ | Shearing force developed at the edges of footing due to shear layer effect |
| $\tau_{f1}$ | Vertical force in punching shear failure plane due to confinement effect |
| $T_R$ | Tensile force mobilised in the reinforcement |
| LDR | Linear density ratio |
| $\Delta Q_{SL}$ | Improvement in bearing capacity due to shear layer effect |
| $\Delta Q_{SL}$ | Improvement in bearing capacity due to confinement effect |
| $\Delta Q_{SL}$ | Improvement in bearing capacity due to additional surcharge effect |
| $L_e$ | Length of reinforcement beyond potential failure surface |
| m | Void depth (ratio of vertical distance from the ground surface to void centre) |
| n | Void eccentricity (ratio of horizontal distances from embankment centreline to void centre) |

## Disclosure statement

No potential conflict of interest was reported by the authors.

## ORCID

Deendayal Rathod http://orcid.org/0000-0001-6290-2913
Kasinathan Muthukkumaran http://orcid.org/0000-0002-7664-7068

## References

AASHTO R. 50-09. 2017. *Recommended Practice for Geosynthetic Reinforcement of the Aggregate Base Course of Flexible Pavement Structures*. Washington, DC: AASHTO.

Abdollahi, M., S. N. Moghaddas Tafreshi, and B. Leshchinsky. 2021. "Protection of Buried Utilities Against Repeated Loading: Application of Geogrid-EPS Geofoam System." *International Journal of Geomechanics* 21 (9): 04021158. doi:10.1061/(asce)gm.1943-5622.0002120.

Abramento, Mauricio, and Andrew J. Whittle. 1995. "Analysis of Pullout Tests for Planar Reinforcements in Soil." *Journal of Geotechnical Engineering* 121 (6): 476–485. doi:10.1061/(ASCE)0733-9410.

Abu-Farsakh, Murad, Shadi Hanandeh, Louay Mohammad, and Qiming Chen. 2016. "Performance of Geosynthetic Reinforced/Stabilized Paved Roads Built Over Soft Soil Under Cyclic Plate Loads." *Geotextiles and Geomembranes* 44 (6): 845–853. Elsevier Ltd. doi:10.1016/j.geotexmem.2016.06.009.

Adams, M. T., and J. G. Collin. 1997. "Large Model Spread Footing Load Tests on Geosynthetic." *Journal of Geotechnical and Geoenvironmental Engineering, ASCE* 123 (1): 66–72. doi:10.1061/(ASCE)1090-0241(1997)123:1(66).

Al Basiouni, Z., Anas Daou, Rana Haj Chhade, and Ghassan Chehab. 2018a. "Experimental and Numerical Assessment of the Behavior of Geogrid-Reinforced Concrete and Its Application in Concrete Overlays." *Journal of Materials in Civil Engineering* 30 (12): 04018332. doi:10.1061/(asce)mt.1943-5533.0002542.

Al Basiouni, Z., Anas Daou, Rana Haj Chhade, and Ghassan Chehab. 2018b. "Experimental and Numerical Assessment of the Behavior of Geogrid-Reinforced Concrete and Its Application in Concrete Overlays." *Journal of Materials in Civil Engineering* 30 (12): 04018332. American Society of Civil Engineers (ASCE). doi:10.1061/(asce)mt.1943-5533.0002542.

Al-Hedad, Abbas S. A., Mengying Zhang, and Muhammad N. S. Hadi. 2020. "Influence of Geogrid Reinforcement on the Drying Shrinkage of High-Strength Concrete Pavements." *Journal of Transportation Engineering, Part B: Pavements* 146 (3): 04020032. doi:10.1061/jpeodx.0000184.

Alimohammadi, Hossein, Junxing Zheng, VR. Schaefer, John Siekmeier, and Raul Velasquez. 2021. "Evaluation of Geogrid Reinforcement of Flexible Pavement Performance: A Review of Large-Scale Laboratory Studies." *Transportation Geotechnics* 27 (September 2020): 100471. Elsevier Ltd. doi:10.1016/j.trgeo.2020.100471.

Aria, Shadi, S. K. Kumar Shukla, and Alireza Mohyeddin. 2020. "Optimum Burial Depth of Geosynthetic Reinforcement Within Sand Bed Based on Numerical Investigation." *International Journal of Geotechnical Engineering* 14 (1): 71–79. Taylor & Francis. doi:10.1080/19386362.2017.1404202.

ASTM. 1995. "Standard Test Method for Determining Tensile Adhesion Properties of Structural." *Test* i: 6–9. doi:10.1520/D6637.

Ayob, Mohamad, Anuar Kasa, Mohd Sofiyan Sulaiman, and Nirwani Devi. 2019. "Slope Stability Evaluations Using Limit Equilibrium and Finite Element Methods Slope Stability Evaluations Using Limit Equilibrium and Finite Element Methods Faculty of." *Ocean Engineering Technology and Informatics, University Malaysia Faculty of Bioengin* 28 (18): 27–43.

Bathurst, R. J., T. M. Allen, Peiyuan Lin, and Nezam Bozorgzadeh. 2019. "LRFD Calibration of Internal Limit States for Geogrid MSE Walls." *Journal of Geotechnical and Geoenvironmental Engineering* 145 (11): 04019087. American Society of Civil Engineers (ASCE). doi:10.1061/(asce)gt.1943-5606.0002124.

Boushehrian, Javad Hajiani, and Nader Hataf. 2003. "Experimental and Numerical Investigation of the Bearing Capacity of Model Circular and Ring Footings on Reinforced Sand." *Geotextiles and Geomembranes* 21 (4): 241–256. doi:10.1016/S0266-1144(03)00029-3.

Bozorgzadeh, Nezam, R. J. Bathurst, T. M. Allen, and Yoshihisa Miyata. 2020. "Reliability-Based Analysis of Internal Limit States for MSE Walls Using Steel-Strip Reinforcement." *Journal of Geotechnical and Geoenvironmental Engineering* 146 (1): 04019119. doi:10.1061/(asce)gt.1943-5606.0002192.

Briançon, L., and B. Simon. 2017. "Pile-Supported Embankment Over Soft Soil for a High-Speed Line." *Geosynthetics International* 24 (3): 293–305. doi:10.1680/jgein.17.00002.

Bs 8006-2010. 2010. "BS 8006," 1: 135–180.

Chakraborty, Manash, and Jyant Kumar. 2014. "Bearing Capacity of Circular Foundations Reinforced with Geogrid Sheets." *Soils and Foundations* 54 (4): 820–832. Japanese Geotechnical Society. doi:10.1016/j.sandf.2014.06.013.

Chaudhary, Babloo, Hemanta Hazarika, Akira Murakami, and Kazunori Fujisawa. 2018. "Geosynthetic-Sheet Pile Reinforced Foundation for Mitigation of Earthquake and Tsunami Induced Damage of Breakwater." *Geotextiles and Geomembranes* 46 (5): 597–610. Elsevier. doi:10.1016/j.geotexmem.2018.04.011.

Chen, Guoyuan. 2009. "A Research on the Dynamical Characteristics of Road-Bridge Transition Sections Reinforced by Geogrid." *GeoHunan International Conference, ASCE*. 60–67. Special publication number 189.

Chen, Jianfeng, Xiaopeng Guo, Rui Sun, Sathiyamoorthy Rajesh, Song Jiang, and Jianfeng Xue. 2021. "Physical and Numerical Modelling of Strip Footing on Geogrid Reinforced Transparent Sand." *Geotextiles and Geomembranes* 49 (2): 399–412. Elsevier Ltd. doi:10.1016/j.geotexmem.2020.10.011.

Chung, Wilson, and Giovanni Cascante. 2007. "Experimental and Numerical Study of Soil-Reinforcement Effects on the Low-Strain Stiffness and Bearing Capacity of Shallow Foundations." *Geotechnical and Geological Engineering* 25 (3): 265–281. doi:10.1007/s10706-006-9109-0.

Correia, N. S., E. R. Esquivel, and J. G. Zornberg. 2018. "Finite-Element Evaluations of Geogrid-Reinforced Asphalt Overlays Over Flexible Pavements." *Journal of Transportation Engineering, Part B: Pavements* 144 (2): 04018020. doi:10.1061/jpeodx.0000043.

Dennes, Bergado, T. By, Associate Member, Lo Kam-Hung, Jin-Chun Chai, Ramaiah Shivashankar, Marolo C Alfaro, and Loren R Anderson. 1992. *Pullout Tests Using Steel Grid Reinforcements with Low-Quality Backfill*. Journal of geotechnical engineering, ASCE.

El Naggar, Hany, Alper Turan, and Arun Valsangkar. 2015. "Earth Pressure Reduction System Using Geogrid-Reinforced Platform Bridging for Buried Utilities." *Journal of Geotechnical and Geoenvironmental Engineering* 141 (6): 04015024. American Society of Civil Engineers (ASCE). doi:10.1061/(asce)gt.1943-5606.0001307.

Eskişar, T., J. Otani, and J. Hironaka. 2012. "Visualization of Soil Arching on Reinforced Embankment with Rigid Pile Foundation Using X-Ray CT." *Geotextiles and Geomembranes* 32: 44–54. doi:10.1016/j.geotexmem.2011.12.002.

Fahel, R. S., Ennio M. Palmeira, and J. A. R. Ortig. 2000. *Behaviour of Geogrid Reinforced Abutments on Soft Soil in the BR 101-SC Highway, Brazil*. Geotechnical Engineering Journal of SEAGS and AGSSEA, ASCE.

Fawaz, Ali. 2014. "Slope Stability Analysis Using Numerical Modelling." *American Journal of Civil Engineering* 2 (3): 60. doi:10.11648/j.ajce.20140203.11.

Fishman, L., K. By, C S. Associate Member, and R L. Sogge. 1993. *Behavior of Instrumented Geogrid Soil Reinforced Wall*. Journal of Geotechnical Engineering, ASCE.

Giroud, J P., M. Asce, and Jie Han. 2004. "Design Method for Geogrid-Reinforced Unpaved Roads." *I Development of Design Method*. doi:10.1061/ASCE1090-02412004130:8775.

Gregory, Monley, J. By, T. H. Jonathan, and Associate Member. 1993. *Tensile Reinforcement Effects on Bridge-Approach Settlement*. Journal of Geotechnical Engineering, ASCE.

Halder, Koushik, and Debarghya Chakraborty. 2018. "Bearing Capacity of Strip Footing Placed on the Reinforced Soil Slope." *International Journal of Geomechanics* 18 (11): 06018025. American Society of Civil Engineers (ASCE). doi:10.1061/(asce)gm.1943-5622.0001278.

Halder, Koushik, and Debarghya Chakraborty. 2019. "Effect of Interface Friction Angle Between Soil and Reinforcement on Bearing Capacity of Strip Footing Placed on Reinforced Slope." *International Journal of Geomechanics* 19 (5): 06019008. American Society of Civil Engineers (ASCE). doi:10.1061/(asce)gm.1943-5622.0001394.

Han, Jie, and Ken Akins. 2002. "Use of Geogrid-Reinforced and Pile-Supported Earth Structures." Deep Foundations, ASCE.

Han, Bingye, Jianming Ling, Xiang Shu, Hongren Gong, Yiren Sun, Andrzej Polaczyk Pawel, Baoshan Huang, and M. Asce. 2018. *Resilient Interface Shear Modulus for Characterizing Shear Properties of Pavement Base Materials*. doi:10.1061/(ASCE)MT.1943.

Han, Bingye, Pawel Polaczyk, Yuetan Ma, Miaomiao Zhang, X. Lu, Fulu Wei, and Baoshan Huang. 2020. "Laboratory Investigation of Critical Factors Affecting Geogrid Reinforcement on Aggregate Base Using Loaded Wheel Tester." *Journal of Transportation Engineering, Part B: Pavements* 146 (4): 04020056. American Society of Civil Engineers (ASCE). doi:10.1061/jpeodx.0000215.

Hosamo, Haidar, Iyad Sliteen, and Songxiong Ding. 2021. "Numerical Analysis of Bearing Capacity of a Ring Footing on Geogrid Reinforced Sand." *Buildings* 11 (2): 1–12. doi:10.3390/buildings11020068.

Indraratna, By B., A. S. Balasubramaniam, and S. Balachandran. 1992. *Performance of Test Embankment Constructed to Failure on Soft Marine Clay*. Journal of Geotechnical Engineering, ASCE.

Indraratna, Buddhima, N. T. Ngo, and Cholachat Rujikiatkamjorn. 2013. "Geogrid Strengthening of an Existing Coal Ash Landfill Cap." *Journal of Geotechnical and Geoenvironmental Engineering* 139 (8): 1275–1289. American Society of Civil Engineers (ASCE). doi:10.1061/(asce)gt.1943-5606.0000864.

Izawa, Jun, and Jiro Kuwano. 2011. "Evaluation of Extent of Damage to Geogrid Reinforced Soil Walls Subjected to Earthquakes." *Soils and Foundations* 51 (5): 945–958. doi:10.3208/sandf.51.945.

Jayalath, Chamara, Chaminda Gallage, Kasun Wimalasena, Jeffrey Lee, and Jothi Ramanujam. 2021. "Performance of Composite Geogrid Reinforced Unpaved Pavements Under Cyclic Loading." *Construction and Building Materials* 304 (April): 124570. Elsevier Ltd. doi:10.1016/j.conbuildmat.2021.124570.

Jayamohan, J., and R. Shivashankar. 2015. "Analytical Modeling of Prestressed Reinforced Granular Beds

Overlying Weak Soils." *National Conference on Furthering Aspirations in Civil Engineering* 1.

Jeon, Han Yong. 2010. "Evaluation of Long-Term Behaviours of Geogrids: A Review." *Proceedings of the Institution of Civil Engineers: Ground Improvement* 163 (4): 189–195. doi:10.1680/grim.2010.163.4.189.

Jiang, Yan, Jie Han, Robert L. Parsons, and James J. Brennan. 2016. "Field Instrumentation and Evaluation of Modular-Block MSE Walls with Secondary Geogrid Layers." *Journal of Geotechnical and Geoenvironmental Engineering* 142 (12): 05016002. American Society of Civil Engineers (ASCE). doi:10.1061/(asce)gt.1943-5606.0001573.

Juran, Han, and Chao L. Chen. 1989. *Strain Compatibility Design Method for Reinforced Earth Walls*. Journal of Geotechnical Engineering, ASCE.

Ke, Han, Ma Pengcheng, Jiwu Lan, Yunmin Chen, and He. Haijie. 2021. "Field Behaviors of a Geogrid Reinforced MSW Slope in a High-Food-Waste-Content MSW Landfill: A Case Study." *Geotextiles and Geomembranes* 49 (2): 430–441. Elsevier Ltd. doi:10.1016/j.geotexmem.2020.10.017.

Khosrojerdi, Mahsa, S. M. Asce, Ming Xiao, M. Asce, Tong Qiu, and Jennifer Nicks. 2019. *Nonlinear Equation for Predicting the Settlement of Reinforced Soil Foundations*. doi:10.1061/(ASCE).

Kumar, Prateek, and Manash Chakraborty. 2020. "Seismic Bearing Capacity of Rough Strip Footing Placed Over Geogrid-Reinforced Two-Layer Sands." *International Journal of Geomechanics* 20 (10): 06020029. American Society of Civil Engineers (ASCE). doi:10.1061/(asce)gm.1943-5622.0001824.

Kumar, Arvind, and Swami Saran. 2003. *Closely Spaced Footings on Geogrid-Reinforced Sand*. doi:10.1061/ASCE1090-02412003129:7660.

Lackner, C., D. T. Bergado, and S. Semprich. 2013. "Prestressed Reinforced Soil by Geosynthetics - Concept and Experimental Investigations." *Geotextiles and Geomembranes* 37: 109–123. Elsevier Ltd. doi:10.1016/j.geotexmem.2013.02.002.

Lai, Fengwen, Fuquan Chen, and D. Li. 2018. "Bearing Capacity Characteristics and Failure Modes of Low Geosynthetic-Reinforced Embankments Overlying Voids." *International Journal of Geomechanics* 18 (8): 04018085. American Society of Civil Engineers (ASCE). doi:10.1061/(asce)gm.1943-5622.0001206.

Liu, H. L., W. W. Ng, M. Asce, and K. Fei. 2007. "Performance of a Geogrid-Reinforced and Pile-Supported Highway Embankment Over Soft Clay: Case Study." *Journal of Geotechnical and Geoenvironmental Engineering*. doi:10.1061/ASCE1090-02412007133:121483.

Mane, A. S., and B. V. S. Viswanadham. 2012. "Studies on the Performance of Geogrid Reinforced Soil Walls with Compressible Inclusion." *Geocongress, ASCE* 2: 1349–1349.

Michael, Adams, T. By, and James G. Collin. 1997. *Large Model Spread Footing Load Tests on Geosynthetic Reinforced Soil Foundations*. 123. Journal of Geotechnical and Geoenvironmental Engineering, ASCE.

Molly, Mathew, and Anand R. Katti. 2014. "Critical Analysis of Internal Stability Methods for Analysis of Reinforced Soil Walls." *International Journal of Civil, Structural, Environmental and Infrastructure Engineering Research and Development (IJCSEIERD)* 4 (2): 47–58. www.tjprc.org/view-archives.php

Nair, Asha Manomohan, and G. Madhavi Latha. 2014. "Cyclic Loading Behaviour of Reinforced Soil-Aggregate Bases." *Proceedings of the Institution of Civil Engineers: Ground Improvement* 167 (2): 88–98. doi:10.1680/grim.12.00007.

Nejad, F. M., Saeid Asadi, Shahab Fallah, and Morteza Vadood. 2016. "Statistical-Experimental Study of Geosynthetics Performance on Reflection Cracking Phenomenon." *Geotextiles and Geomembranes* 44 (2): 178–187. Elsevier Ltd. doi:10.1016/j.geotexmem.2015.09.002.

Oser Cihan, C., S. F. Cinicioglu, and Ozer Cinicioglu. 2020. "Design Method for Quantifying Embankment Safety Against Lateral Spreading and Determining Contribution of Basal Reinforcements." *Geotextiles and Geomembranes* 48 (3): 297–305. Elsevier. doi:10.1016/j.geotexmem.2019.12.002.

Park, Young Jin, Mohammed A. Gabr, Roy H. Borden, Kyung Jun Kim, and Christopher A Kreider. 2007. "Limit Equilibrium and Deformation Analyses of a Geogrid-Reinforced Embankment." *Geosynthetics in Reinforcement and Hydraulic Applications, ASCE.*

Pham, T. A., and Daniel Dias. 2021. "3D Numerical Study of the Performance of Geosynthetic-Reinforced and Pile-Supported Embankments." *Soils and Foundations* 61 (5): 1319–1342. Japanese Geotechnical Society. doi:10.1016/j.sandf.2021.07.002.

Qian, Jinsong, Xinran Chen, Chen Jin, and Wei Fu. 2018. "Influence of Combined Load on the Performance of Geosynthetics as Antireflective Cracking System in Semirigid Base Asphalt Pavements." *Journal of Materials in Civil Engineering* 30 (9): 04018222. American Society of Civil Engineers (ASCE). doi:10.1061/(asce)mt.1943-5533.0002446.

Qian, Yu, Jie Han, S. K. Pokharel, and R. L. Parsons. 2013. "Performance of Triangular Aperture Geogrid-Reinforced Base Courses Over Weak Subgrade Under Cyclic Loading." *Journal of Materials in Civil Engineering* 25 (8): 1013–1021. American Society of Civil Engineers (ASCE). doi:10.1061/(asce)mt.1943-5533.0000577.

Qian, Yu, Jie Han, Sanat K. Pokharel, Robert L. Parsons, M S. Student Research Assistant, and Ph D Candidate. 2010. *Experimental Study on Triaxial Geogrid-Reinforced Bases Over Weak Subgrade Under Cyclic Loading*. GeoFlorida: Advances in Analysis Modeling and Design, ASCE.

Qu, Honglue, Xue Huang, Yanan Gao, Zhe Zhang, and Chenxu Wang. 2022. "Shaking Table Test of Subgrade Slope Reinforced by Gravity Retaining Wall with Geogrids." *Earthquake Engineering and Engineering Vibration* 21 (3): 715–727. doi:10.1007/s11803-022-2108-1.

Ragui Wilson-Fahmyfl Robert, M., F. Koerner, Honorary Member, and Leonard J. Sansone. 2012. *Experimental Behavior of Polymeric Geogrids in Pullout*. Journal of Geotechnical Engineering, ASCE.

Rajesh, S., and B. V. S. Viswanadham. 2012. "Centrifuge Modeling and Instrumentation of Geogrid-Reinforced Soil Barriers of Landfill Covers." *Journal of Geotechnical and Geoenvironmental Engineering* 138 (1): 26–37. American Society of Civil Engineers (ASCE). doi:10.1061/(asce)gt.1943-5606.0000559.

Rajesh, S., and B. V. S. Viswanadham. 2014. *Numerical Simulation of Geogrid-Reinforced Soil Barriers Subjected to Differential Settlements*. doi:10.1061/(ASCE)GM.1943.

Ravi, K., S. K. Kumar Dash, Stefan Vogt, and G. Braeu. 2014. "Behaviour of Geosynthetic Reinforced Unpaved Roads

Under Cyclic Loading." *Indian Geotechnical Journal* 44 (1): 77–85. doi:10.1007/s40098-013-0051-9.
Robinson, W. Jeremy, I. L. Howard, J. S. Tingle, and GJ. Norwood. 2020. "Analysis of Full-Scale Geosynthetic Reinforced Airfield Pavement Subjected to Accelerated Aircraft Loading." *Journal of Transportation Engineering, Part B: Pavements* 146 (3): 04020052. American Society of Civil Engineers (ASCE). doi:10.1061/jpeodx.0000212.
Romeo, D., P. Pezzano, and P. Rimoldi. 2022. "Short-Term Design of Geosynthetic-Reinforced Embankments on Soft Foundation Soils." *IOP Conference Series: Materials Science and Engineering* 1260 (1): 012001. doi:10.1088/1757-899x/1260/1/012001.
Rowe, R. Kerry, and A. L. Li. 2005. "Geosynthetic-Reinforced Embankments Over Soft Foundations." *Geosynthetics International* 12 (1): 50–85. doi:10.1680/gein.12.1.50.59424.
Safaee, A. M., Ahmad Mahboubi, and Ali Noorzad. 2021. "Experimental Investigation on the Performance of Multi-Tiered Geogrid Mechanically Stabilized Earth (MSE) Walls with Wrap-Around Facing Subjected to Earthquake Loading." *Geotextiles and Geomembranes* 49 (1): 130–145. Elsevier Ltd. doi:10.1016/j.geotexmem.2020.08.008.
Saha, Roy, and Kousik Deb. 2019. Influence of Footing Interference on Bearing Capacity Improvement for Geogrid-Reinforced Sand Bed Underlain by Soft Clay. Geo-Congress, ASCE.
Saha, S., and Kousik Deb. 2020. "Effect of Aspect Ratio of Footing on Behavior of Two Closely-Spaced Footings on Geogrid-Reinforced Sand." *Geotextiles and Geomembranes* 48 (4): 443–453. Elsevier. doi:10.1016/j.geotexmem.2020.02.003.
Saha Roy, S., and K. Deb. 2017. "Effects of Aspect Ratio of Footings on Bearing Capacity for Geogrid-Reinforced Sand Over Soft Soil." *Geosynthetics International* 24 (4): 362–382. doi:10.1680/jgein.17.00008.
Samadhiya, N. K., Priti Maheshwari, Attila Zsaki, Partha Basu, and Ayan Kundu. 2009. "Strengthening of Clay by Geogrid Reinforced Granular Pile." *International Journal of Geotechnical Engineering* 3 (3): 377–386. doi:10.3328/IJGE.2009.03.03.377-386.
Saran, Swami, K. G. Garg, and R. K. Bhandari. 1992. *Retaining Wall with Reinforced Cohesionless Backfill.* Journal of Geotechnical Engineering, ASCE.
Sawwaf, M., and AK. Nazir. 2010. "Behavior of Repeatedly Loaded Rectangular Footings Resting on Reinforced Sand." *Alexandria Engineering Journal* 49 (4): 349–356. Faculty of Engineering, Alexandria University. doi:10.1016/j.aej.2010.07.002.
See Keung, Ho, and R. Kerry Rowe. 1994. *Predicted Behavior of Two Centrifugal Model Soil Walls.* Journal of Geotechnical Engineering, ASC.
Silva Vieira, Castorina, and P. M. Pereira. 2021. "Short-Term Tensile Behaviour of Three Geosynthetics After Exposure to Recycled Construction and Demolition Materials." *Construction and Building Materials* 273: 122031. Elsevier Ltd. doi:10.1016/j.conbuildmat.2020.122031.
Sireesh, S., T. G. Sitharam, and S. K. Kumar Dash. 2009. "Bearing Capacity of Circular Footing on Geocell-Sand Mattress Overlying Clay Bed with Void." *Geotextiles and Geomembranes* 27 (2): 89–98. doi:10.1016/j.geotexmem.2008.09.005.
Sridharan, A., B. R. Srinivasa Murthy, and K. Revanasiddappa. 1991. *Technique for Using Fine-Grained Soil in Reinforced Earth.* Journal of GeotechnicalEnineering, ASCE.
Tan, Xin, Zhengbo Hu, Changfu Chen, and Minghua Zhao. 2021. "3D DEM-FDM Coupled Analysis of the Behavior of an Isolated Geogrid-Encased Stone Column Under Axial Loading." *Journal of Geotechnical and Geoenvironmental Engineering* 147 (6): 04021028. doi:10.1061/(asce)gt.1943-5606.0002516.
Tutumluer, Erol, Hai Huang, and Xuecheng Bian. 2012. "Geogrid-Aggregate Interlock Mechanism Investigated Through Aggregate Imaging-Based Discrete Element Modeling Approach." *International Journal of Geomechanics* 12 (4): 391–398. doi:10.1061/(asce)gm.1943-5622.0000113.
Useche-Infante, Danny, Gonzalo Aiassa Martinez, Pedro Arrúa, and Marcelo Eberhardt. 2022. "Experimental Study of Behaviour of Circular Footing on Geogrid-Reinforced Sand." *Geomechanics and Geoengineering* 17 (1): 45–63. Taylor & Francis. doi:10.1080/17486025.2019.1683621.
Wang, H. L., and R. P. Chen. 2019. "Estimating Static and Dynamic Stresses in Geosynthetic-Reinforced Pile-Supported Track-Bed Under Train Moving Loads." *Journal of Geotechnical and Geoenvironmental Engineering* 145 (7): 04019029. doi:10.1061/(asce)gt.1943-5606.0002056.
Wang, J. Q., L. L. Liang Zhang, J. F. Feng Xue, and Yi Tang. 2018. "Load-Settlement Response of Shallow Square Footings on Geogrid-Reinforced Sand Under Cyclic Loading." *Geotextiles and Geomembranes* 46 (5): 586–596. Elsevier. doi:10.1016/j.geotexmem.2018.04.009.
Wang, Y. L., X. Z. Zhuang Cui, Jin Li, Lei Wang, J. W. Li, and Jun wei Su. 2021. "Pullout Behavior of Sensor-Enabled Geobelts in Weathered Rock Material–Granulated Rubber Mixtures." *Geotechnical and Geological Engineering* 39 (1): 499–515. Springer International Publishing. doi:10.1007/s10706-020-01509-w.
Xiao, Ming, Jan Bowen, Mathew Graham, and Jesus Larralde. 2012. "Comparison of Seismic Responses of Geosynthetically Reinforced Walls with Tire-Derived Aggregates and Granular Backfills." *Journal of Materials in Civil Engineering* 24 (11): 1368–1377. doi:10.1061/(asce)mt.1943-5533.0000514.
Xie, Yonggui, Ben Leshchinsky, and Jie Han. 2019. "Evaluation of Bearing Capacity on Geosynthetic-Reinforced Soil Structures Considering Multiple Failure Mechanisms." *Journal of Geotechnical and Geoenvironmental Engineering* 145 (9): 04019040. American Society of Civil Engineers (ASCE). doi:10.1061/(asce)gt.1943-5606.0002072.
Xu, Fang, Hossein Moayedi, L. K. Foong, Mohamad Jamali Moghadam, and Milad Zangeneh. 2021. "Laboratory and Numerical Analysis of Geogrid Encased Stone Columns." *Measurement: Journal of the International Measurement Confederation* 169 (June 2020): 108369. Elsevier Ltd. doi:10.1016/j.measurement.2020.108369.
Xu, Hua, Xin Ren, Jian-Nan Chen, Lei Xia, and Zi-Yun Chen. 2019. *Field Test and Numerical Analysis on Geogrid-Reinforced Slope with High Embankment on Top.* Geo-Congress, ASCE.
Yadu, Laxmikant, and R. K. Tripathi. 2014. "Effect of Depth and Number of Layers of Reinforcement on Bearing Capacity Ratio of Strip Footing Resting on Granulated Blast Furnace Slag Reinforced with Geogrid." Geo-Congress, ASCE.

Yoo, Chungsik, and Qaisar Abbas. 2019. "Performance of Geosynthetic-Encased Stone Column-Improved Soft Clay Under Vertical Cyclic Loading." *Soils and Foundations* 59 (6): 1875–1890. Japanese Geotechnical Society. doi:10.1016/j.sandf.2019.08.006.

Zhang, J., J. J. Zheng, and Y. E. Lu. 2014. "Evaluation of the New Technique of Geogrid-Reinforced and Pile-Supported Embankment at Bridge Approach." *Journal of Bridge Engineering* 19 (4): 06014001. American Society of Civil Engineers (ASCE). doi:10.1061/(asce)be.1943-5592.0000568.

Zhao, Mengxuan, Chunyuan Liu, Tahar El-Korchi, Haichao Song, and Mingjiang Tao. 2019. "Performance of Geogrid-Reinforced and PTC Pile-Supported Embankment in a Highway Widening Project Over Soft Soils." *Journal of Geotechnical and Geoenvironmental Engineering* 145 (11): 06019014. doi:10.1061/(asce)gt.1943-5606.0002157.

Zhao, L. S., W. H. Zhou, Xueyu Geng, K. V. Yuen, and Behzad Fatahi. 2019. "A Closed-Form Solution for Column-Supported Embankments with Geosynthetic Reinforcement." *Geotextiles and Geomembranes* 47 (3): 389–401. Elsevier. doi:10.1016/j.geotexmem.2019.01.006.

Zheng, Yewei, A. C. Sander, Wenyong Rong, P. J. Fox, P. Benson Shing, and J. S. McCartney. 2018. "Shaking Table Test of a Half-Scale Geosynthetic-Reinforced Soil Bridge Abutment." *Geotechnical Testing Journal* 41 (1): 171–192. doi:10.1520/GTJ20160268.

Zhou, Yang, and Gangqiang Kong. 2019. "Deformation Analysis of Geosynthetic-Encased Stone Column–Supported Embankment Considering Radial Bulging." *International Journal of Geomechanics* 19 (6): 04019057. doi:10.1061/(asce)gm.1943-5622.0001426.

Zhuang, Yan, and Xiaoyan Cui. 2016. "Case Studies of Reinforced Piled High-Speed Railway Embankment Over Soft Soils." *International Journal of Geomechanics* 16 (2): 2. doi:10.1061/(asce)gm.1943-5622.0000519.

Zhuang, Y., and E. A. Ellis. 2016. "Finite-Element Analysis of a Piled Embankment with Reinforcement and Subsoil." *Geotechnique* 66 (7): 596–601. doi:10.1680/jgeot.15.P.139.

Zhuang, Yan, and Kangyu Wang. 2018. "Finite Element Analysis on the Dynamic Behavior of Soil Arching Effect in Piled Embankment." *Transportation Geotechnics* 14: 8–21. Elsevier Ltd. doi:10.1016/j.trgeo.2017.09.001.

Zidan, A. F. 2012. "Numerical Study of Behavior of Circular Footing on Geogrid-Reinforced Sand Under Static and Dynamic Loading." *Geotechnical and Geological Engineering* 30 (2): 499–510. doi:10.1007/s10706-011-9483-0.